

## FRACTURE TOUGHNESS OF SIMULATED H.A.Z.

G. Bernard, L. Devillers, F. Faure\*, B. Marandet

Institut de Recherches de la Sidérurgie Française (IRSID)  
185, Rue du Président Roosevelt 78105 Saint Germain-en-Laye (France)

### ABSTRACT

The heat affected zone (H.A.Z.) is often considered to be a privileged site for the initiation of brittle fracture. The narrowness of this coarse-grained zone, its proximity to more ductile structures and its often irregular contours unfortunately constitute major obstacles to the precise location of a notch for laboratory testing. For these reasons, we were led to measure the inherent fracture toughness of heat affected zones, not on real welded joints but on massive structures simulated by heat treatment or on finite-width structures simulated by means of the Gleeble R.P.L. machine. Measurements of  $J_{Ic}$  carried out at different temperatures on fatigue precracked compact tension specimens confirm the existence of a correlation between fracture toughness transition temperature ( $TK_{Ic}$ ) and impact transition temperature (TK 28). Moreover, it appears that the surrounding of the brittle zone by more ductile structures has the effect of increasing the apparent fracture toughness.

Finally, we propose the general application of a model which, thanks to knowledge of the mechanical parameters relative to loading (residual stress field, applied load) and the toughness properties of the different metallurgical structures involved ( $J_{Ic}$  of H.A.Z., R-curve of base metal) makes it possible to evaluate quantitatively the critical flaw size and its subsequent evolution within the structure.

### KEYWORDS

Welding ; Heat Affected Zone ; J-integral ; initiation ; microstructures ; fracture ; residual stresses.

### INTRODUCTION

Toughness measurements of the various zones of a welded joint, specially of the Heat Affected Zone (H.A.Z.) is a problem the answer to which has not been clearly stated yet. Experiments conducted on Charpy specimens show that simulated H.A.Z. microstructures display different abilities to withstand brittle fracture (Bernard, Faure and Gauthier, 1976). However, it appears clearly that measuring H.A.Z. toughness with the help of Charpy tests is not a fully accepted procedure. Owing to the narrowness of the studied zone which is of the same order of magnitude as the blunt notch itself, it can be considered that the toughness measurements are altered by the effect of neighbouring structures. Furthermore this test does not clearly separate crack initiation from crack propagation. Therefore we may have to resort to toughness tests which make use of perfectly located, extremely fine notches (fatigue cracks). Among such tests we have selected the J-integral method whose ability to test H.A.Z. and assess critical flaw sizes will be presented here.

\* - Now with FRAMATOME, Service Matériaux, Cedex 16, 92084 PARIS La Défense.

## SIMULATION OF HEAT AFFECTED ZONE STRUCTURES

The material studied is a Mo-Nb 20 mm thick tube type steel whose composition and mechanical properties are indicated in Table 1.

TABLE 1 - Chemical composition and mechanical properties of the material studied.

Chemical composition (weight percent)					
C	Mn	Si	Al	Mo	Nb
0,160	1,470	0,325	0,039	0,210	0,043
Tensile properties at room temperature					
$\sigma_{ys}$ (N/mm <sup>2</sup> )	$\sigma_{ut}$ (N/mm <sup>2</sup> )	Elongation (%)	Reduction in Area (%)		
535	695	24	63		

$J_{Ic}$  fracture toughness tests were performed on simulated homogeneous H.A.Z. structures obtained by salt bath heat treatments followed by controlled cooling in proper quenching media and simulated H.A.Z. obtained by means of the Gleeble R.P.I. machine. The Gleeble simulated specimens display a few millimeters wide H.A.Z. enclosed by base metal. This situation is very much similar to the one of a real H.A.Z. enclosed by base and weld metal.

#### Salt Bath Heat Treatments

Specimens blank were heated at 1250°C for 10 mn and given the following treatments :

- water quenching (cooling parameter  $\Delta t_{300}^{700} \leq 5$  s) yielding a fully martensitic structure ;
- oil quenching ( $20 \text{ s} \leq \Delta t_{300}^{700} \leq 30$  s) yielding a mixture of martensite and lower bainite ;
- quenching into an aqueous solution of methyl cellulose ( $\Delta t_{300}^{700} \approx 350$  s) yielding upper bainite ;
- air cooling ( $\Delta t_{300}^{700} \approx 1000$  s) yielding a mixture of coarse bainite and ferrite.

Each of these structures is representative of H.A.Z. obtained with different welding energies. Their mechanical properties are given in Table 2.

TABLE 2 - Mechanical properties of H.A.Z. Structures.

	Hardness		Tensile Properties				Charpy Properties	
	$\Delta t_{300}^{700}$ (s)	HV5	$\sigma_{ys}$ (N/mm <sup>2</sup> )	$\sigma_{ut}$ (N/mm <sup>2</sup> )	Elongation (%)	Reduction in Area(%)	TK 28J (°C)	FATT (°C)
Water quenching	$\leq 5$	410	980	1200	12	54	0	+10
Oil quenching	30	385	800	1130	13	52	-35	-20
Methyl cellulose quenching	300	220	470	700	23	63	+30	+40
Air cooling	1000	210	465	690	22	58	+40	+70
Gleeble specimens	300	240	545	700	-	-	+30	+60

#### Gleeble R.P.I. Heat Treatments

The specimens initially  $11 \times 16 \times 95 \text{ mm}^3$  in size were machined into  $10 \times 15 \times 80 \text{ mm}^3$  ( $B \times W \times L$ ) notched three point bend bars. We have chosen a 300 seconds cooling parameter ( $\Delta t_{300}^{700} = 300$  s or  $\Delta t_{500}^{800} = 80$  s), typical of high energy welding and similar to that obtained by quenching into an aqueous solution of methyl cellulose. The mechanical properties of this material are indicated in Table 2 above. To study the effect of neighbouring more ductile structures, we have prepared samples with H.A.Z. widths ranging from 5 to 30 mm.

EXPERIMENTAL DETERMINATION OF  $J_{Ic}$ 

After heat treating, the following test specimens were prepared :

- in the salt bath treated blanks, 15 mm thick compact tension specimens ;
- in the Gleeble treated blanks,  $10 \times 15 \text{ mm}^2$  (cross-section) three point bend specimens.

All specimens were longitudinal with respect to rolling direction and notches perpendicular to the plate surface. Test specimens were fatigue precracked following the ASTM E399 specification but for the crack length (a) which was such that  $0.6 \leq \frac{a}{W} \leq 0.7$ .

J-integral was calculated from the load, load-point displacement curve, using the modified Merkle and Corten (1974) derivation :

$$J = \frac{A}{B(W-a)} f\left(\frac{a}{W}\right) \quad (1)$$

where A = area under load, load-displacement record in energy units

B = specimen thickness

a = original crack size

$(W-a)$  = initial uncracked ligament

$f\left(\frac{a}{W}\right)$  = dimensionless coefficient value given in a table (Clarke and Landes, 1979).  
For the three-point bend specimen,  $f\left(\frac{a}{W}\right) = 2$ .

The critical  $J_{Ic}$  value was determined at initiation of ductile stable crack growth by the A.C. potential drop method developed at IRSID (Marandet and Sanz, 1977 a ; Marandet and co-workers, 1978). The corresponding fracture toughness value  $K_{Jc}$  was derived from  $J_{Ic}$  according to the expression :

$$K_{Jc} = \sqrt{\frac{E}{(1-\nu^2)} J_{Ic}} \quad (2)$$

where E = Young's modulus (206.000 MPa)

$\nu$  = Poisson's ratio (0.3)

## RESULTS

### Salt Bath Heat Treated Specimens

Figure 1 shows that for all four different structures  $K_{Jc}$  increases with increasing temperature, reaches a maximum and then decreases in most cases. This is associated with a transition of the fracture mode. Different record types corresponding to the most typical fracture modes are schematically described on Fig.2. At low temperature, one gets a set of discontinuities of various extends corresponding to Fig.2 (a), (b) or (c). Each discontinuity is associated with cleavage unstable crack growth. Initiation of ductile crack extension is detected at the minimum of the potential displacement curve. Above a given temperature fracture occurs by a fully ductile mechanism (Fig.2-d). Recent investigations (Marandet, Phelippeau, Rousse-lier, 1980) show that in this later case,  $J_{Ic}$  depends on the dimensions of the specimen (B, W-a). Thus we decided to take into consideration only  $J_{Ic}$  measurements performed within the cleavage initiation range. In this range the requirement ( $W-a$ ),  $B \geq 50 \frac{J_{Ic}}{\sigma_{ys}}$  is always fulfilled up to  $-40^\circ\text{C}$  for oil quenched structures. Note that at this temperature  $K_{Jc}$  toughness reaches  $130 \text{ MPa}\sqrt{\text{m}}$ . All other structures allow valid  $J_{Ic}$  measurements up to room temperature (Fig.1).

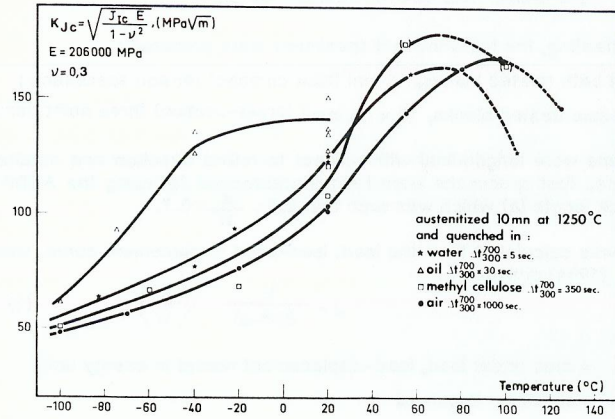


Fig. 1. Fracture toughness  $K_{Jc}$  as a function of temperature for various H.A.Z. microstructures.

Gleeble R.P.I. Heat Treated Specimens ( $\Delta t_{300} = 300$  s)

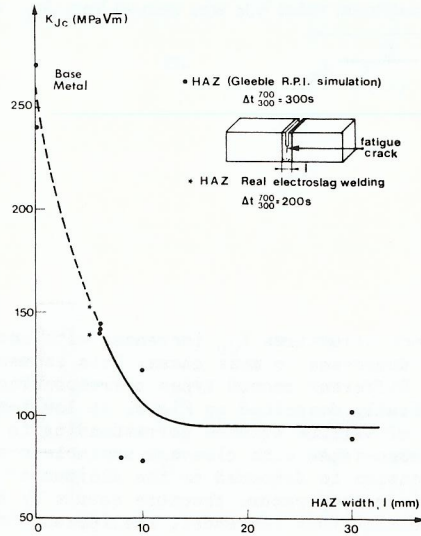
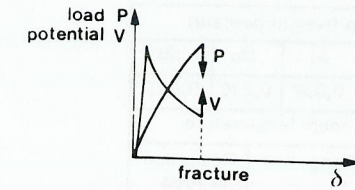
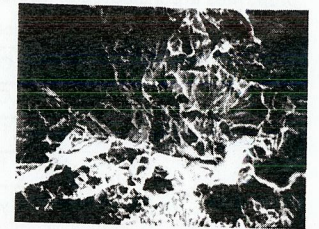


Fig. 3. Fracture toughness  $K_{Jc}$  as a function of the H.A.Z. width.

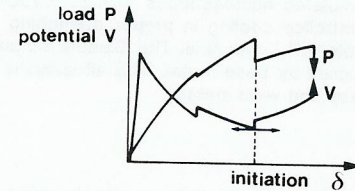
Figure 3 shows the fracture toughness  $K_{Jc}$  as a function of the H.A.Z. width for a cooling parameter  $\Delta t_{300} = 300$  s. It clearly appears that  $K_{Jc}$  is significantly increased when the width of the H.A.Z. becomes smaller than 6 mm. The same effect has been observed recently by Schmidtman (1979) on the Charpy impact toughness of Gleeble simulated H.A.Z.. As pointed out by this author, the "supporting effect" of the more ductile adjacent structures can only be observed if the plastic zone extends out of the H.A.Z.. Actually the critical H.A.Z. width would depend on temperature and yield strength of the H.A.Z. structure.



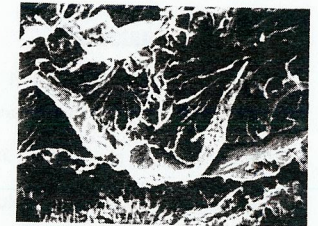
(a)



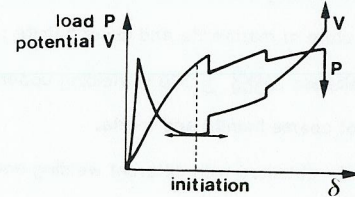
x 270



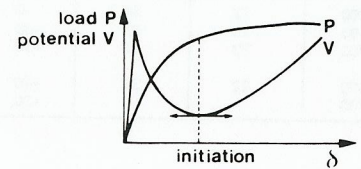
(b)



x 400



(c)



(d)



x 240

Fig. 2. Typical diagrams recorded at different temperatures.

Relationship Between Fracture Toughness and Charpy Impact Transition Temperatures

A linear relationship between Charpy impact transition temperature defined at a 28J level and fracture toughness transition temperature defined at a 100 MPa√m level, has been pointed out for base metal by Marandet and Sanz (1977). Both transition temperatures obtained in this study are displayed on Fig. 4 as a function of the cooling parameter  $\Delta t_{300}$ . It appears that fracture toughness and Charpy impact tests yield the same structure grading. The lower transition temperatures are associated with composite structures (martensite-bainite), the higher with coarser structures (upper bainite, ferrite-carbides) which are brought about by high energy welding. These results suggest that a linear relationship, similar to that established previously for base metal, can be derived for H.A.Z. structures.

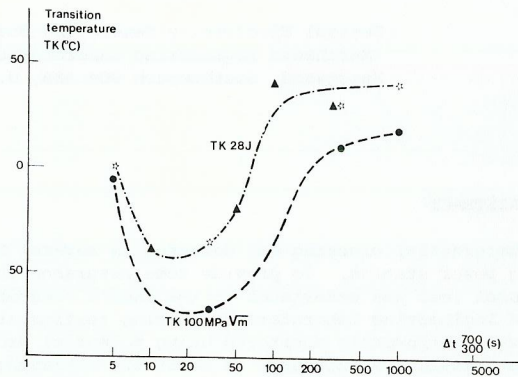


Fig. 4. Comparison between fracture toughness transition temperature (TK 100 MPa√m, °C) and impact transition temperature (TK 28J, °C) for different simulated H.A.Z. microstructures.

THEORETICAL APPROACH TO FRACTURE OF A WELDED JOINT

We discuss here the fracture mechanisms of a welded joint taking our inspiration from a recent paper by Masubuchi (1977). We will describe the model set up by this author and we will try to extend it with the help of the  $J_{Ic}$  and R-curve concepts.

Masubuchi's Model

Let us consider an infinite plate, subjected to a uniform stress  $\sigma$ , with a crack of length  $l = 2a$  at its center (Fig. 5-a). The relationship between  $a$  and the crack extension force  $G_I$  is for plane strain conditions :

$$G_I = \sigma^2 \pi a \frac{(1-\nu^2)}{E} \quad (3)$$

This is the equation of the OA1 straight line on Fig. 5-a. Fracture toughness of the material is measured by the critical crack extension force  $G_{Ic}$ , thus brittle fracture will occur for a crack length  $l_c$ . Let us now consider the case where a welded joint runs across the plate in the direction of the main applied stress. The welded joint introduces a residual stress field described schematically on Fig. 5-b. The through thickness defect of half length  $a$  is still perpendicular to the main stress and is lying in the as welded weld metal. Under such circumstances, the crack extension force  $G_I$  is mainly dependent upon residual stress intensity at the crack tip and upon the residual stress field within the plate.  $G_I$  values have been derived by Kihara and Masubuchi (1959) and Kihara (1972) as a function of the defect half length. The crack extension curve ( $G_I$ - $a$ ) goes through a maximum ( $\beta_1$ ) which is dependent on the magnitude of the residual

stresses and becomes tangent (B1) to the straight line OA1 when it goes out of the stress affected area. Assuming that  $G_{Ic}$  is a material constant, brittle fracture will be initiated by a defect ( $l_{r1}$ ) smaller than the critical flaw size ( $l_c$ ) of the first plate.

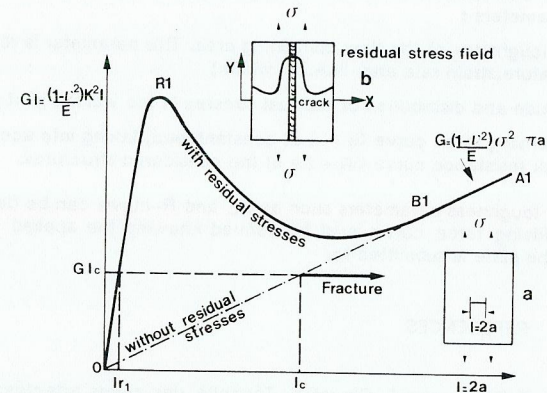


Fig. 5. Graphical model of brittle fracture initiation for a center crack panel under controlled load :  
 a) without residual stresses (base metal)  
 b) with residual stresses (welded joint).  
 (after Masubuchi, 1977).

Extension of the Model

The Masubuchi's model can be helpful to predict initiation of an unstable cleavage fracture in the weld metal or Heat Affected Zone. However it does not predict the further propagation or arrest of this crack within the base metal which can be predicted from the crack extension Resistance curve or R-curve. This concept is considered nowadays as a material toughness parameter for given thickness, temperature and loading rate (Marandet and Sanz, 1977).

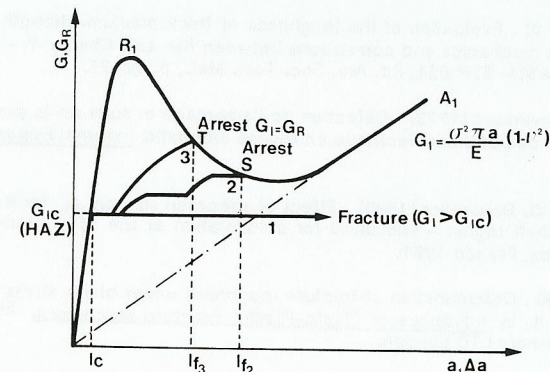


Fig. 6. Graphical model of fracture initiation and propagation for a welded center crack panel with residual stresses. Brittle fracture initiates in the welded joint (Weld Metal or H.A.Z.) and further propagates or arrests in the Base metal.

As shown on Fig. 6 a crack initiated by cleavage in the weld metal or H.A.Z. characterized by a  $G_{Ic}$  (or  $J_{Ic}$ ) value can propagate in the base metal in any of the following modes :

- up to complete fracture (curve number 1) since  $G_I$  is always larger than  $G_{Ic}$  ;
- by consecutive cleavage and ductile steps (curve number 2) and stop at point S where  $G_I = G_R$ . The total magnitude of crack growth is then  $l_{f2} - l_c$  ;
- by stable ductile crack growth (curve number 3) and stop at point T, where  $G_I = G_R$ . The total magnitude of propagation is then  $l_{f3} - l_c$ .

## CONCLUSION

To assess the critical flaw size in a brittle area of a welded joint (H.A.Z. or weld metal) and the further crack extension or arrest in the neighbouring weld metal one has to take into account the following parameters :

- $G_{Ic}$  or  $J_{Ic}$  toughness of the flaw containing area. This parameter is related to metallurgical structure, temperature, strain rate and H.A.Z. width ;
- the magnitude and distribution of residual stresses in the welded joint ;
- the crack driving force curve  $G_I - a$  at constant load, taking into account the residual stress field and the crack resistance curve  $G_R - \Delta a$  of the considered structures.

The fracture toughness parameters such as  $J_{Ic}$  and R-curve can be determined experimentally but the crack driving force curve must be derived knowing the applied stress field and the residual stress field the plate is submitted to.

## REFERENCES

- Bernard, G., F. Faure, and G. Gauthier. Ténacité des zones affectées par la chaleur de soudage des aciers au C-Mn et microalliés. In External Report IRSID RE 374, June 1976.
- Clarke, G.A., and J.D. Landes (1979). Evaluation of the J integral for the compact specimen. Journal of Testing and Evaluation, 7, (5), p. 264-269.
- Kihara, H., K. Masubuchi, T. Kusuda, and K. Iida (1959). Initiation and propagation of brittle fractures in residual stress fields. Documents X-219-59, Commission X of the International Institute of Welding.
- Kihara, H. (1972). Researches on brittle fracture initiation of welded steel structures in Japan. Japan Welding Engineering Society, Tokyo, July 1972.
- Marandet, B., and G. Sanz (1977 a). Experimental verification of the  $J_{Ic}$  and equivalent energy methods for the evaluation of the fracture toughness of steels. In Flaw Growth and Fracture, ASTM STP 631, Ed. Am. Soc. Test. Mat., p. 462-476.
- Marandet, B., and G. Sanz (1977 b). Evaluation of the toughness of thick medium-strength steels by using linear-elastic fracture mechanics and correlations between  $K_{Ic}$  and Charpy V - notch. In Flaw Growth and Fracture, ASTM STP 631, Ed. Am. Soc. Test. Mat., p. 72-95.
- Marandet, B., G. Labbe, and co-workers (1978). Détection de l'amorçage et suivi de la propagation d'une fissure par variation du potentiel électrique en régime alternatif. External Report IRSID RE 549, June 1978.
- Marandet, B., G. Phelippeau, and G. Rousselier (1980). Effect of specimen size on  $J_{Ic}$  for a Ni-Cr-Mo rotor steel in the upper shelf region - submitted for presentation at the fifth international conference on fracture, Cannes, France 1981.
- Marandet, G., and G. Sanz (1979). Determination of fracture toughness under plane stress conditions by the R-curve method. In Advances in Elasto-Plastic Fracture Mechanics, Ed. L.H. Larsson Applied Science Publishers LTD London.
- Masubuchi, K. (1977). Similarities among theories of residual stress, joint restraint and fracture mechanics, Documents IX-1054-77 and X-871-77 of the International Institute of Welding.
- Schmidtman, E. (1979). Influence of the structure on the toughness properties of the heat affected zone of welds of the high-strength fine-grained structural steels StE 36 and StE 47. Stahl u. Eisen, n° 3, February, p. 106-112.